Functional Materials 18, No.1 (2011) © 2011 — STC "Institute for Single Crystals"

Mechanism of AlN film formation at thermochemical nitridization of sapphire

Kh.Sh.-ogly Kaltaev, S.V.Nizhankovskiy, N.S.Sidelnikova, M.A.Rom, A.Ya.Danko, M.V.Dobrotvorskaya, A.Ye.Belyaev, V.V.Strelchuk*, A.F.Kolomys**

Institute for Single Crystals, STC "Institute for Single Crystals", National Academy of Sciences of Ukraine, 60 Lenin Ave., 61001 Kharkiv, Ukraine
*V. Lashkaryov Institute of Semiconductor Physics, National Academy of Sciences of Ukraine, 41 Nauky Ave., 03028 Kyiv, Ukraine

Received July 23, 2010

The results of studying the mechanism of AlN film formation on sapphire substrates with the orientation relations at $(000\bar{1})AlN//(0001)Al_2O_3$, $(0001)AlN//(11\bar{2}0)Al_2O_3$, $(10\bar{1}3)AlN//10\bar{1}0)Al_2O_3$ and $(11\bar{2}0)AlN//(10\bar{1}2)Al_2O_3$ at the thermochemical nitridization of sapphire in $N_2 + (CO, H_2)$ reducing atmospheres are presented. It is shown that the main defects in the obtained films are predominantly related to with the presence of elevated concentration of oxygen in these films. A possible mechanism of nitridization which comprises reducing and diffusion processes, is discussed.

Представлены результаты исследований механизма формирования пленок AlN на сапфировых подложках с ориентационными соотношениями $(0001)AlN//(0001)Al_2O_3$, $(0001)AlN//(11\bar{2}0)Al_2O_3$, $(10\bar{1}3)AlN//(10\bar{1}0)\ Al_2O_3$ и $(11\bar{2}0)AlN//(10\bar{1}2)Al_2O_3$ при термохимической нитридизации сапфира в восстановительных средах $N_2 + (CO, H_2)$. Показано, что основные дефекты в полученных пленках преимущественно связаны с наличием в них повышенной концентрации кислорода. Обсуждается возможный механизм нитридизации, включающий восстановительные и диффузионные процессы.

1. Introduction

Combined AlN/Al_2O_3 substrates (templates) are an alternative for expensive crystalline aluminum nitride substrates used for epitaxy of AlGaN/GaN heterostructures to be applied as a base for creation of light emitting diodes (LED), laser diodes and elements of SHF electronics. By now, there have been developed many physicochemical methods for the obtaining of AlN/Al_2O_3 templates. AlN films on sapphire surface are produced by the methods of magnetron sputtering, molecular beam epitaxy (MBE), metallorganic chemical vapor deposition (MOCVD) and hydride vapor phase epitaxy (HVPE).

Establishment of the main regularities in the transformation of sapphire into the phases in the system $AlN–A_2O_3$ at nitridization of sapphire using gaseous reducing agents (CO, H_2) [1] made it possible to propose a new method of sapphire nitridization and of the obtaining of aluminum nitride films by annealing sapphire substrate in a gas mixture $N_2 + (CO, H_2)$ [2]. Thereat, in contrast to the above-mentioned methods, aluminum nitride film is formed on the surface of sapphire due to dissolution of nitrogen in anion-deficient corundum and subsequent crystallochemical transformations in a surface-adjacent layer of sapphire substrate [2].

In the present work, we consider the mechanism of the formation of aluminum nitride film in the process of annealing of

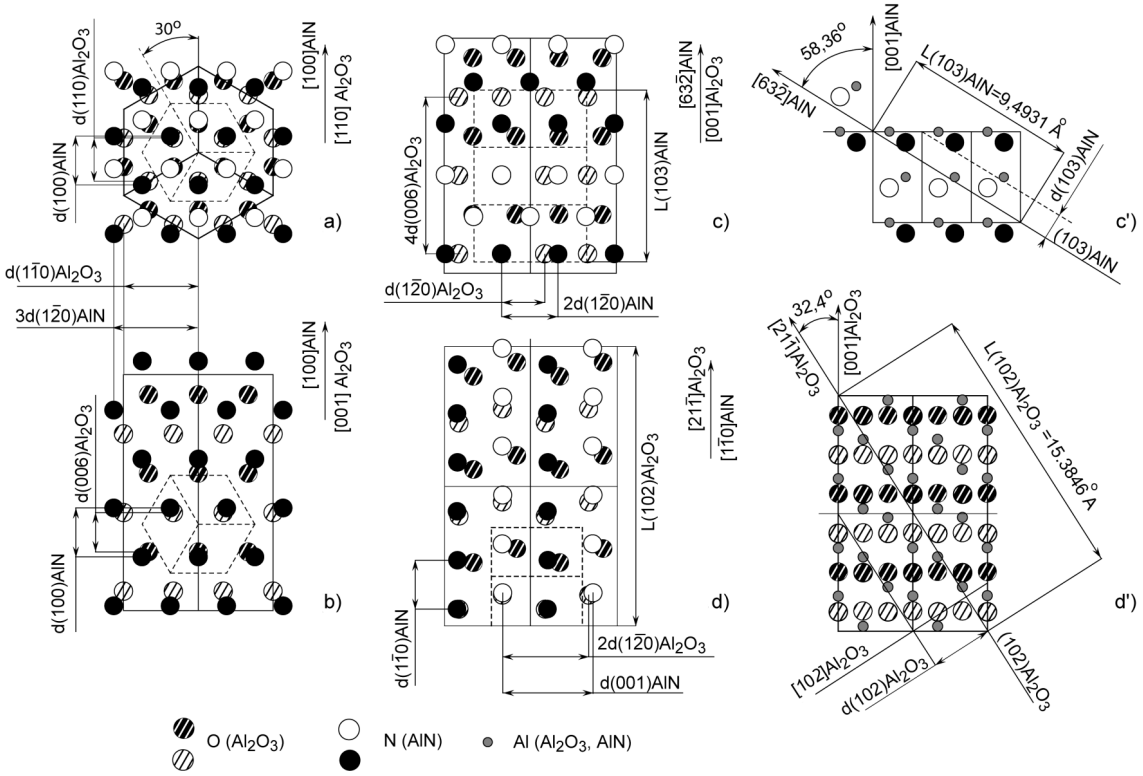

Fig. 1. Schemes of orientation relations for: (0001)AlN/(0001)Al_2O_3 — (a), (0001)AlN/(11$\bar{2}$0)Al_2O_3 — (b), (10$\bar{1}$3)AlN/(10$\bar{1}$0)Al_2O_3 — (c) and (10$\bar{2}$0)AlN/(10$\bar{1}$2)Al_2O_3 — (d); (c′), (d′) is the position of (10$\bar{1}$3) plane in AlN lattice and of (10$\bar{1}$2) plane in Al_2O_3 lattice, respectively.

sapphire substrate in nitrogen-containing reducing atmosphere, and establish the dependence of the optical and luminescent characteristics of this film on the conditions of its obtaining.

2. Objects and methods of investigation

To obtain AlN films we used 1 mm thick polished plane-parallel sapphire substrates with a diameter of 25.4 mm and (0001), (10$\bar{1}$0), (11$\bar{2}$0) and (10$\bar{1}$2) crystallographic orientations of the surface. The surface roughness (R_a) was ~2 nm, the deviation of the crystallographic axis from the normal to the surface ranged between 15′ and 1°. The process of annealing was realized in a furnace with carbon-graphite thermal screens which provided creation of reducing conditions at temperatures of 1300–1850°C. The furnace was preliminarily heated up to 1100°C under the conditions of forevacuum pumping. At a residual pressure of ~10–30 Pa the chamber was filled with nitrogen or $CO_2 + N_2$ mixture to achieve a pressure of 1.05–1.25 atm, and then the furnace temperature was raised up to the required value. The concentration of CO and H_2 in the gaseous medium was controlled by means of a gas chromatograph "Crystal 2000M". The temperature was measured using an integral infrared pyrometer Marathon MRISCSF. The process of annealing lasted from 10–20 min. to 24 h. X-ray phase analysis was realized on a diffractometer DRON-1.5 in $CuK\alpha_{1,2}$ radiation (monochromator — pyrographite (002)) according to the scheme θ–2θ. The thickness of the crystalline film (x) was determined both in the approximation of homogeneous screen attenuating the crystal reflections [3], and from the intensity of their interference lines in the symmetric Bragg geometry [4]. At the measurement of the rocking curves the angles α were found to be 1–8° (DRON-3 diffractometer, $CuK\alpha_1$ radiation, Ge (111) monochromator, (n, $-m$) scheme).

3. Discussion of results

Studies of the process of substrate nitridization show that the thickness, the profile of the distribution of the elements in the film, as well as its structure perfection depend on the temperature, annealing time and partial pressure of the components in

Table 1. Characteristics of lattices mismatch Al_2O_3 and AlN

Orientation (film//substrate)	Directions in Al_2O_3 lattice	Equivalent elements		$M = \frac{d_{AlN} - d_{Al_2O_3}}{d_{Al_2O_3}} \cdot 100$, %
		AlN (Å)	Al_2O_3 (Å)	
(0001)AlN//(0001)Al_2O_3	[110]*	d(100) (2.6942)	d(110) (2.3791)	13.24
	[1$\bar{1}$0]*	3d(1$\bar{2}$0) (4.6665)	d(1$\bar{1}$0) (4.1207)	13.24
	[001]**	d(002) (2.4895)	d (2.1652)	14.98
(0001)AlN//(11$\bar{2}$0)Al_2O_3	[1$\bar{1}$0]*	3d (1$\bar{2}$0) (4.6665)	d(1$\bar{1}$0) (4.1207)	13.24
	[001]*	d(100) (2.6942)	d(006) (2.1652)	24.43
	[110]**	d(002) (2.4895)	d(110) (2.3791)	4.64
(10$\bar{1}$3)AlN//(1000)Al_2O_3	[001]*	L(103) (9.4931)	4d(006) (8.6607)	9.61
	[1$\bar{2}$0]*	2d(1$\bar{2}$0) (3.111)	d(1$\bar{2}$ (2.3791)	30.76
	[100]**	3d(103) (4.2387)	d(100) (4.1207)	2.86
(11$\bar{2}$0)AlN//(10$\bar{1}$2)Al_2O_3	[21$\bar{1}$]*	d(1$\bar{1}$0) (2.6942)	(102)/6 (2.5641)	5.07
	[1$\bar{2}$0]*	d(001) (4.979)	2d (1$\bar{2}$0) (4.7582)	4.64
	[1052]**	3d(110) (4.6665)	d(102) (3.4795)	34.11

* — in the film surface, ** — in the direction of the transformed layer growth.

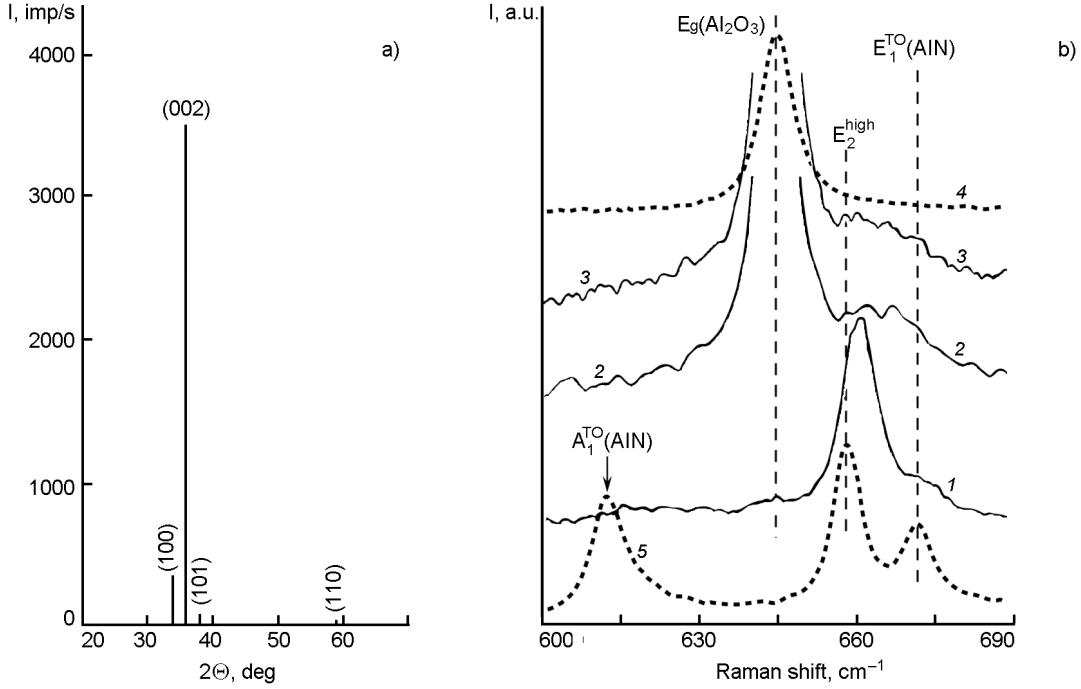

Fig. 2. (a) — X-ray pattern (Cu $K\alpha_{1,2}$ radiation) for 250 nm thick AlN/Al_2O_3 with the texture (001). (b) — Raman spectra of the samples: (0001)AlN(250 nm)/(0001)Al_2O_3 — *1*, (0001)AlN(25 nm)/(10$\bar{2}$0) Al_2O_3 — *2*, (0001)AlN(30 nm)/(10$\bar{2}$0)Al_2O_3 — *3*, Al_2O_3 _ *4* and of the massive sample AlN [9] — *5*.

the mixture. The film surface roughness (R_a) does not exceed 5 nm.

The orientation relations AlN//Al_2O_3 determined by the method of X-ray diffractometry are the following: (0001)AlN//(0001)Al_2O_3, (0001)AlN//(11$\bar{2}$0)Al_2O_3, (10$\bar{1}$3)AlN//(10$\bar{1}$0)Al_2O_3 (11$\bar{2}$0)AlN//(10$\bar{1}$2)Al_2O_3 (Fig. 1). It should be noted that the relations we obtained for AlN on (0001), (11 (11$\bar{2}$0), (10$\bar{1}$2) sapphire substrates are also characteristic of other methods and coincide with the results reported in [5, 6]. Moreover, in the literature there are also available the data on other orientation relations such as (10$\bar{1}$0)AlN//(10$\bar{1}$0)A_2O_3 [5], AlN(11$\bar{2}$2)//(1$\bar{1}$00)A_2O_3 [7].

It has been established that for the obtaining of (0001)AlN/Al_2O_3, the orientation (11$\bar{2}$0) of the initial substrate is preferable, in spite of more essential discrepancy of the lattices in the substrate plane. In this case

Table 2. Frequency position and half-width of A_1^{TO}, E_2^{high}, E_1^{TO} phonon lines

	Bulk AlN [8]	(0001)AlN (250 nm)/(0001)Al_2O_3		(0001)AlN (30 nm)/(11$\bar{2}$0)Al_2O_3		(0001)AlN (25 nm)/(11$\bar{2}$0)Al_2O_3	
	Energy, cm^{-1}	Energy, cm^{-1}	FWHM, cm^{-1}	Energy, cm^{-1}	FWHM, cm^{-1}	Energy, cm^{-1}	FWHM, cm^{-1}
A_1^{TO}	608.5	615.5	16.8	—	—	—	—
E_2^{high}	655.5	659.5	7.3	659.2	≈15.8	659.7	≈12.2
E_1^{TO}	669.3	669.8	14.1	669.4	≈11.1	669.7	≈11.3

the diffraction patterns show the presence of the peak AlN(002) only. If there are used the substrates of the orientation (0001), the diffraction patterns contain, besides the peak AlN(002), the peaks (100), (101), (110) with intensities lower than 0.01 of that of the main peak (Fig. 2a), which testifies to the presence of crystallites of another orientation in the layer.

Fig. 2a presents the X-ray pattern (Cu $K\alpha_{1,2}$ radiation) of 250 nm thick AlN film with the texture (001) (RWHM $\beta \approx 1.1°$, the reflection (002), Cu $K\alpha_1$ radiation) obtained on (0001)Al_2O_3 and annealed in CO + N_2 mixture (CO<0.1 vol.%) at 1400°C during 10 h. The Raman spectrum of this sample and those of the samples (0001)AlN/(11$\bar{2}$0)Al_2O_3 with a thickness of 25 and 30 nm ($\beta \approx 0.65°$) obtained under similar conditions on the substrates are shown in Fig. 2b. Presented there for comparison are the Raman spectra of unstrained massive AlN sample [8] and Al_2O_3 (substrate).

The Raman scattering studies were carried out in the geometry of back scattering at scanning along the wurtzite axis (Z-direction). The spectra were measured by means of a spectrometer T64000 Jobin Yvons. As an excitation source, there was used the 488.0 nm line of Ar^+/Kr^+ laser Spectra Physics Stability 2018-RM. The beam power varied within 0.25–25 mWt range. The samples were placed on a surface which allowed positioning of the excitation in the plane XY. The exciting beam was focused in the depth of the structure by a piezoelectric controller to an accuracy of 0.1 μm. A microscope of Olympus BX41 type with 100X magnification (the aperture NA = 0.90) was used for laser beam focusing and scattered light collection. The frequency positions and the values of the phonon line half-widths are presented in Table 2.

In the spectra there are registered the phonon line E_2^{high} of AlN with hexagonal structure, as well as a weak scattering line E_1^{TO} (AlN) forbidden by the selection rules and testifying to structure distortions in AlN layer. For the sample (0001)AlN(250 nm)/(0001)Al_2O_3 the shift of the phonon line E_2^{high} by $\Delta\nu = 4$ cm^{-1} ($\nu(E_2^{high}) = 659.5$ cm^{-1}) towards higher frequencies is due to compression strains in the film plane [9, 10].

The presence of compression strains in ALN film is also confirmed by the measurement of the lattice constants performed on a DRON-3 diffractometer (Cu $K\alpha_1$ radiation) by the Bond method from the reflections (006) and (114) in the film with a thickness of ≈50 μm. The obtained values $a = 3.0993 \pm 0.0004$ Å, $c = 4.989 \pm 0.0006$ Å ($c/a = 1.6097$) differ from the corresponding parameters $a = 3.111$ Å, $c = 4.979$Å ($c/a = 1.60045$) characteristic of the AlN film produced by nitridization of highly dispersed Al_2O_3 powders [1]. As is known, similar changes of the lattice constants also occur at other methods of the obtaining of AlN films, and are connected with compression strains in the film plane and stretching strains in the perpendicular direction [11, 12].

The samples (0001)AlN/(11$\bar{2}$0)Al_2O_3 with 25 and 30 nm thick AlN films show not only the shift of the maximum towards higher frequencies, but also the broadening of the phonon line E_2^{high} up to 12–16 cm^{-1} (Table 2). This seems to be caused by structure distortions, in particular, by an elevated content of oxygen in the lattice of AlN [10, 13]. It should be noted that though the FWHM values of the line E_2^{high} typical of the investigated films (≈7–16 cm^{-1}) exceed the corresponding value for massive defect-free AlN single crystal (3 cm^{-1}) [14], they are considerably lower than the one observed in the crystals with a high content of defects (~50 cm^{-1}) [15].

As mentioned above, the thickness of the obtained films depends on the partial pressure of the components in the annealing atmosphere, the annealing temperature and duration. The film which has the crystal lattice of AlN is formed after 10–15 min of the annealing. The minimum annealing du-

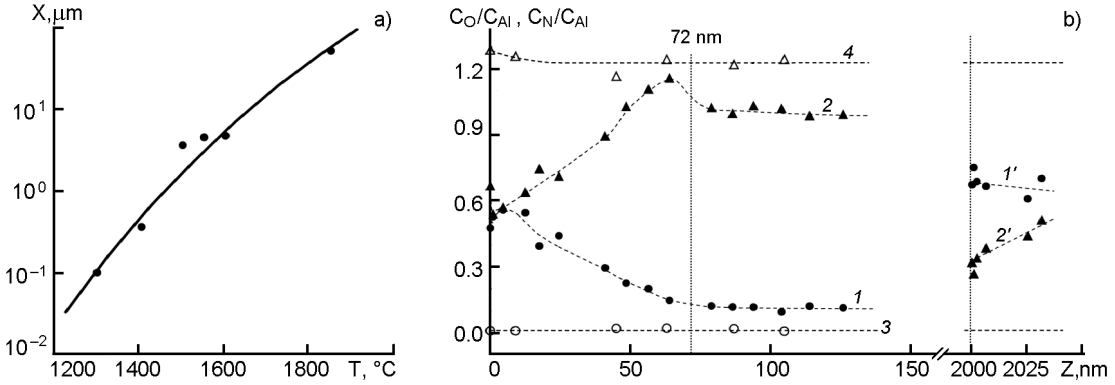

Fig. 3.(a) Dependence of the maximum film thickness on the annealing temperature (the annealing duration is 10 h): experimental data (points) and the calculated dependence $x = \sqrt{D \cdot T}$, ($D = 5 \cdot 10^6 \cdot \exp(-6.591/k \cdot T)$ $cm^2 \cdot c^{-1}$). (b) — Relative distribution of the elements in the depth: *1*, *1′*, *3* — C_N/C_{Al}, *2*, *2′*, *4* — C_O/C_{Al}, *1*, *2* — in the sample (0001)AlN(72 nm)/(0001)Al_2O_3, *1′*, *2′* — in the sample (0001)AlN(50 μm)/(0001)Al_2O_3 (at a distance of ≈2 μm from the surface), *3*, *4* — in the reference sapphire sample.

ration is limited by the response time of the furnace. When the composition of the mixture (N_2, CO, CO_2, H_2, H_2O) and the temperature are fixed, with the increase of the annealing time from 10–15 minutes to ≈10 hours the dependence of the film thickness (x) on the annealing duration (t) is parabolic [2]. This testifies to the fact that the film growth mechanism is predominantly diffusive ($x=\sqrt{D \cdot t}$). If the annealing lasts 10 h, the maximum film thickness rises with the temperature from less than 1 μm at 1300–1400°C up to ≈50 μm at 1850°C (Fig. 3a). The minimum x values obtained by changing the composition of the annealing atmosphere essentially (up to an order of magnitude) differ from the maximum values. The annealing longer than 10 h is not accompanied with further noticeable rise of the film thickness [2]. For the investigated temperature interval, the values of effective diffusion coefficient obtained on the base of the maximum experimental x values (determined by X-ray diffraction method) and t obtained for (0001)AlN/(0001)Al_2O_3 to a sufficient accuracy (Fig. 3a, Table 3), are described by the relation:

$$D_{eff} \approx 5 \cdot 10^6 \cdot \exp(-6.591/k \cdot T), \quad (1)$$

D_{eff} value is intermediate between those of the diffusion coefficient of anionic vacancies [16, 17] and oxygen [18, 19] in Al_2O_3 lattice (Table 3).

In [20] the effective diffusion coefficient at sapphire nitridization in NH_3 atmosphere at 1100°C is estimated using the method of X-ray photoelectron spectroscopy. The obtained value (≈10^{-16} $cm^2 \cdot s^{-1}$) exceeds the one determined by means of relation (1) more than by an order of magnitude.

The diffusion character of the film formation is also confirmed by the components distribution profile in the depth of the film (Fig. 3b). The composition of the surface layer of the sapphire substrate subjected to nitridization was determined by the method of X-ray photoelectron spectroscopy using a

Table 3. Diffusion coefficients ($cm^2 \cdot s^{-1}$) for anionic and oxygen vacancies (literature data) and D_{eff} values (experimental data)

T, °C	D_V = $430 \cdot \exp(-80/R \cdot T)$ [17]	D_O = $6.8 \cdot \exp(-6.1/k \cdot T)$ [19]	D_{eff} = $5 \cdot 10^6 \cdot \exp(-6.591/k \cdot T)$	$D_{exp} = x^2/t$
1300	$3.25 \cdot 10^{-9}$	1.9·10–19	3.82·10–15	2.78·10–15
1400	$1.5 \cdot 10^{-8}$	2.86·10–18	$6.99 \cdot 10^{-14}$	$3.4 \cdot 10^{-14}$
1500	$5.84 \cdot 10^{-8}$	$3.11 \cdot 10^{-17}$	$9.21 \cdot 10^{-13}$	$3.6 \cdot 10^{-12}$
1550	$1.09 \cdot 10^{-7}$	$9.31 \cdot 10^{-17}$	$3.01 \cdot 10^{-12}$	$5.63 \cdot 10^{-12}$
1600	$1.96 \cdot 10^{-7}$	$2.63 \cdot 10^{-16}$	$9.21 \cdot 10^{-12}$	$5.88 \cdot 10^{-12}$
1850	$2.47 \cdot 10^{-6}$	$2.25 \cdot 10^{-14}$	$1.13 \cdot 10^{-9}$	$6.94 \cdot 10^{-10}$

XSAM-800 Kratos spectrometer. The vacuum in its chamber was of about 10^{-5} Pa. Photoelectrons were excited by MgK_α radiation ($h\nu = 1253.6$ eV). The sample surface composition was established form the area ratio for the O1s, Al2p, N1s lines of the skeleton shells taking into account the sensitivity coefficients. The depth of the analyzed layer was ~5 nm. The profile of the elements distribution in the film depth was determined by means of layer-by-layer analysis with ionic etching (Ar^+, $E = 1.5$ keV, the etching rate = 1 nm/min). The spectra were calibrated with respect to the C1s line ($E_{sv.} = 285$ eV) of the hydrocarbons adsorbed by the surface. The bonding energy values observed for the main lines of the skeleton shells of the elements (O1s:E_{bond} = 531.8 eV, Al2p:E_{bond} = 74.0 eV, N1s:E_{bond} = 397.2 eV) testify to the presence of the chemical bonds Al–N, Al–O. One can distinguish a minor non-uniformity for the N1s line ($E_{bond} = 399.2$ eV) with an intensity not exceeding 10 % of that of the main peak, which may be caused by the bonds Al–O–N.

Fig. 3b presents the results of layer-by-layer analysis of the samples with films of different thickness. Before examining the sample with ≈50 μm thick film (curves *1'*, *2'*), a portion of the film with a thickness of ~2 μm was removed by chemico-mechanical polish.

As seen from Fig. 3b, the film composition quietly approaches an equilibrium level at the boundary between the film and the matrix. Moreover, at a depth essentially exceeding the film thickness the concentration of nitrogen is higher and the concentration of oxygen is lower in comparison with those of the reference sapphire sample. On the other hand, the formed film contains relatively high oxygen concentration which depends on the distance from the phase boundary, and has practically linear distribution of the ratios of the components' concentrations in its depth (curves *1*, *2*). Formally, the film may be considered a solid solution of varying composition $(AlN)_x(Al_2O_3)_{1-x}$ (with AlN structure), where $x = 0.8$–0.9 in the vicinity of the surface and linearly decreases to 0.3 at the wurtzite-corundum phase boundary. It is to be noted that, according to the phase diagram of the system AlN–Al_2O_3, the composition with $x \approx 0.3$ corresponds to the oxynitride phase of the spinel γ-AlON. Obviously, such a distribution of the components is equilibrium for the AlN films obtained by sapphire nitridization.

Analysis of the above data makes it possible to assume the presence of two main stages in the process of film formation. In our opinion, at the initial stage limited by the mobility of anionic vacancies, the composition of the surface layer becomes non-stoichiometric, and nitrogen starts diffusing into the bulk of sapphire. This process is accompanied with the formation of $Al_2O_{3-\delta}$:N solid solution with corundum structure in the diffusion region. When a certain critical composition of the solution is achieved in a local volume, the oversaturated solution decomposes in the layer which depth is essentially less than the one of the diffusion region. This is followed by the formation of the nuclei of the phases AlON, AlN which are equilibrium for such conditions; then they grow irreversibly by absorbing the initial phase molecules. Thereat, we assume that the oxygen excessive for the equilibrium composition of the formed phase is rejected by the growing phase boundary, and penetrates, in particular, into the bulk of the Al_2O_3 matrix. Inside the matrix, it forms a barrier layer (with an elevated oxygen concentration) which limits the rate of the growth of the nitride layer into the bulk of sapphire. The distance between the barrier layer and the surface depends on the extent of Al_2O_3 non-stoichiometry and, consequently, on the reducing properties of the annealing atmosphere. An indirect evidence of the appearance of the barrier layer is an elevated content of oxygen near the phase boundary (Fig. 3b, curve *2*).

Thus, we assume that the fastest process of nucleation limited by the mobility of anionic vacancies lasts several minutes after the beginning of the annealing; then the thickness of the film increases at a lower rate which is limited mainly by the rate of oxygen diffusion from the barrier layer.

It is obvious that the formation of AlN film also depends on the choice of the annealing atmosphere composition (partial pressures of N_2, CO, CO_2, H_2 and H_2O in the mixture) which provides the conditions for realization of the reactions:

$$Al_2O_3(s) + 3CO(g) + N_2(g) \rightarrow 2AlN(s) + 3CO_2(g), \quad (2)$$

$$Al_2O_3(s) + 3H_2(g) + N_2(g) \rightarrow 2AlN(s) + 3H_2O(g), \quad (3)$$

i.e. stability of the phase formed.

According to this mechanism, the concentration of oxygen in the film essentially depends on the extent of Al_2O_3 non-

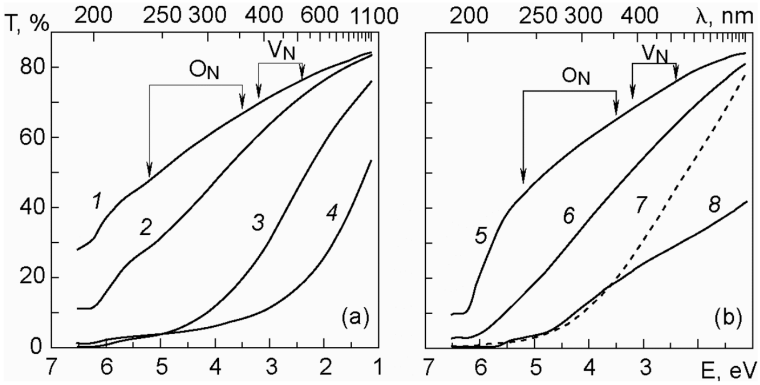

Fig. 4. Optical transmission spectra for (0001) AlN/(0001)Al_2O_3. The curve denotations correspond to the order numbers of the investigated samples (Table 4).

Table 4. Production conditions and structure characteristics of (0001)AlN/(0001)Al_2O_3 obtained at annealing in CO + N_2 gaseous mixture

No.	*T*, °C	Annealing time, h	CO concentration in the mixture, vol.%	Film thickness, nm	FWHM β, deg. (reflection (002), Cu $K\alpha_1$ radiation)
1	1400	10	<0.1	72	1.1
2	1400	10	0.23*	70	2.5
3	1500	10	<0.1	500	2
4	1500	10	<0.1*	600	3.5
5	1400	10	<0.1	270	0.6
6	1400	10	0.15	240	1.1
7	1400**	10**	0.1	130	1.1
8	1850	10	3.2	$\approx 5 \cdot 10^4$	0.4

* while obtaining the 2nd and 4th samples, the regeneration ability of graphite was reduced by partial screening,

** while obtaining the 7th sample, at the end of annealing the temperature was raised by 150°, and additional annealing was realized during 1 hour under the same conditions

stoichiometry at the initial stage of the film formation. As known from the literature, the presence of oxygen in the lattice of AlN considerably influences its structure perfection, thermal conductivity, electrophysical, optical and other properties [21–24]. Therefore, the reducing properties of the medium belong to the main parameters which define the functional properties of the produced films.

Fig. 4 presents the transmission spectra $T(\lambda)$ of (0001)AlN/(0001)Al_2O_3 obtained at the annealing of the films in a gaseous mixture CO + N_2 under different conditions. The conditions of the obtaining of AlN films and their structural characteristics are shown in Table 4. The optical density of the samples was measured on a Perkin-Elmer Lambda-35 spectrophotometer at 190–1100 nm wavelengths.

According to the data reported in [24–26], the absorption bands in the ≈250–600 nm range (≈5.2–2.5 eV) are connected with the presence of structure defects in the AlN lattice. The band with a maximum at 2.8–2.9 eV is referred to nitrogen vacancies, whereas the 3.5–5.2 eV absorption region is defined by the presence of oxygen in the lattice. The maximum of this band is shifted from ≈4.3 eV at low oxygen concentrations to ≈4.8 eV at high concentrations. These defects and the luminescent characteristics of AlN are being actively investigated nowadays in view of the use of such crystals in thermoluminescent detectors of ionizing radiation, on a level with Al_2O_3:C crystals (anion-deficient corundum which main dosimetric peak is observed within the same temperature interval [27]). As reported in the mentioned paper, the luminescence peak with a maximum at 2.58 eV (480 nm — blue light emission) is caused by the inherent defects, i.e. nitrogen vacancies, whereas the peak at

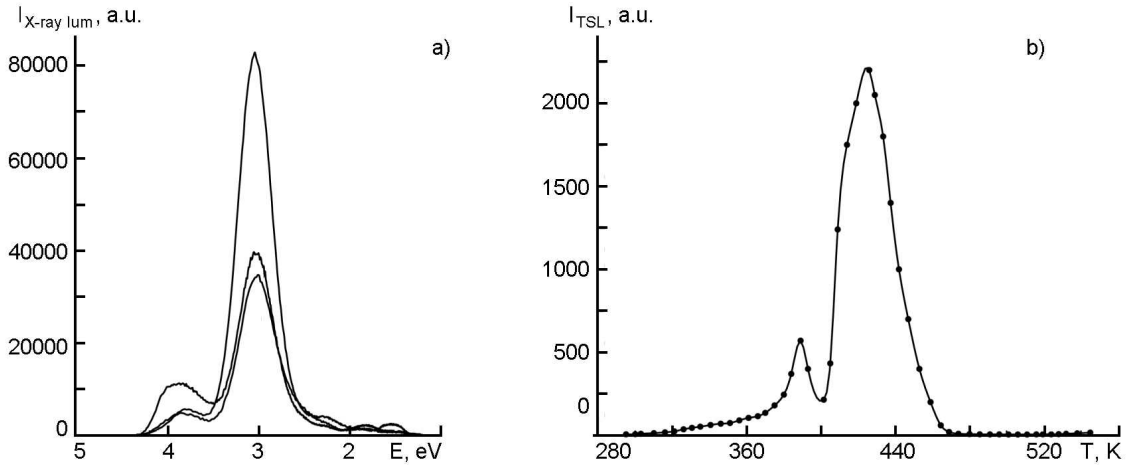

Fig. 5. Spectra of X-ray luminescence (a) and thermoluminescence (heating rate is 5 deg./min) (b). The curve denotations correspond to the order numbers of the investigated samples (Table 1).

≈3.09 eV (400 nm — violet light emission) is due to the complexes V_{Al}–O_N–3N and V_{Al}–$2O_N$–2N (O_N denotes oxygen in the position of nitrogen, V_{Al} is aluminum vacancy).

For the films with a thickness less than 1 μm a correlation is observed between the structure perfection, absorption intensity in the region of the said defects and the reduction potential of the medium used for the obtaining of the films. Taking into account the film thickness, the maximum transmission value in the 2.5–5.2 eV range is observed for the 1st and the 5th samples formed at the minimum concentration of CO in the gaseous mixture. As this concentration rises, the transmission in the said region of the spectrum diminishes. The same effect also takes place at forced decrease of the regeneration ability of graphite which leads to the increase of the ratio P_{CO_2}/P_{CO} in the annealing medium (curves *1*, *2* and *3*, *4*). It is interesting to compare the characteristics of the 6th and the 7th samples obtained under identical conditions with $\beta = 1.1°$. However, the film thickness of the latter sample subjected to additional annealing at higher temperatures decreases, and the transmission in the 2.5–5.2 eV range essentially lowers. This may be caused by the fact that the additional annealing at a temperature of 1550°C has given rise to more intense dissolution of the barrier layer created at the initial stage of the formation of the film, and to oxygen diffusion from the matrix into the film.

It should be also noted that, taking into account the thickness (≈50 μm), the 8th sample is characterized by rather high transmission in the 3.5–5.2 eV range, which correlates with the content of oxygen in it (Fig. 3b).

The peaks bound up with the presence of structure defects are also observed in the spectra of X-ray- and thermoluminescence (Fig. 5) measured at excitation with an X-ray tube REIS (U = 30 kV, I = 50 μA, Cu-anticathode), FEU-100 photomultiplier used as a radiation receiver. The intensity of the X-ray luminescence peaks correlates with the one of the corresponding absorption bands in the spectra $T(\lambda)$ (Fig. 4).

4. Conclusions

The method of sapphire nitridization in nitrogen-containing reducing atmosphere allows the obtaining of AlN films with a thickness ranging between 20–30 nm to ≈50 μm on sapphire substrates with the orientations $(000\bar{1})AlN//(000\bar{1})Al_2O_3$, $(000\bar{1})AlN//(11\bar{2}0)Al_2O_3$, $(10\bar{1}3)AlN//(10\bar{1}0)Al_2O_3$, $(11\bar{2}0)AlN//(10\bar{1}2)Al_2O_3$).

The nature of the main defects in the obtained films is defined mainly by the presence of elevated oxygen concentrations. The optical transmission spectra $T(\lambda)$ of the films contain the absorption bands in ≈250–600 nm range (≈5.2–2.5 eV), bound up with the presence of structure defects in the lattice of AlN (nitrogen vacancies and vacancies of oxygen in the position of nitrogen). There is established a correlation between the absorption intensity in the region of the said defects and the reduction potential of the medium used for the obtaining of the film. The peaks bound up with the presence of structure defects are also observed in the X-ray and thermoluminescence spectra.

The proposed model of the process of the formation of AlN film at thermochemical ni-

tridization of sapphire consists of several stages. The first stage which lasts several minutes after the beginning of the annealing, is characterized by a violation of the surface layer stoichiometry, and nitrogen diffusion into the bulk of sapphire with consequent formation of $Al_2O_{3-\delta}$:N solid solution with the structure of corundum in the diffusion area. Then in the region of the solid solution (with a thickness considerably less than the diffusion length) the process of nucleation followed by the formation and growth of AlN film with elevated concentration of oxygen develops at the boundary AlN-matrix (barrier layer). At the next stage, further annealing leads to the increase of the film thickness at a lower rate limited by the rate of the diffusion from the barrier layer.

References

1. A.Y.Dan'ko, M.A.Rom, N.S.Sidel'nikova et al., *Functional Materials*, **14**, 460 (2007).
2. Kh.Sh.-ogly Kaltaev, N.S.Sidel'nikova, S.V.Nizhankovskiy et al., *Semiconductors*, **43**, 1606 (2009).
3. E.F.Chaikovsky, In Apparatuses and Methods of X-ray Analysis, 1st issue, Mashinostroenie, Leningrad (1967), 186 [in Russian].
4. N.S.Greshnyakova, V.G.Alekseev, V.N.Egorov et al., In Apparatuses and Methods of X-Ray Analysis, 21st issue, Mashinostroenie, Leningrad (1978),122 [in Russian].
5. J.Meinschien, F.Falk, R.Hergt, H.Stafast, *Appl. Phys.*, **A 70**, 215 (2000).
6. C.J.Sun, P.Kung, A.Saxler et al., *J. Appl. Phys.*, **75**, 3964 (1994).
7. L.Lahourcade, E.Bellet-Amalric, E.Monroy, *Appl. Phys. Lett.*, **90**, 131909 (2007).
8. A.R.Goni, H.Siegle, K.Syassen et al., *Phys. Rev.*, **B 64**, 35205 (2001).
9. H.J.Trodahl, F.Martin, P.Muralt, N.Setter, *Appl. Phys. Lett.*, **89**, 061905 (2006).
10. V.Lughia, D.R.Clarke, *Appl. Phys. Lett.*, **89**, 241911 (2006).
11. Z.Y.Fan, G.Rong, J.Browning et al., *Mater. Sci. Eng.*, **B 67**, 80 (1999).
12. Q.X.Guo, K.Yahata, T.Tanaka et al., *J. Cryst. Growth*, **257**, 123 (2003).
13. E.F.McCullen, J.S.Thakur, Y.V.Danylyuk et al., *J. Appl. Phys.*, **103**, 063504 (2008).
14. K.Kuball, J.M.Hayes, Ying Shi, J.H.Edgar, *Appl. Phys. Lett.*, **77**, 1958 (2000).
15. P.Perlin, A.Polian, T.Suski, *Phys. Rev.*, **B 47**, 2874 (1993).
16. A.Ya.Danko, N.S.Sidelnikova, G.T.Adonkin et al., *Poverkhnost: Roentgen., Synkhrotron. and Neutron Issled.*, **9**, 44 (2004).
17. T.P.Jones, R.L.Coble, C.J.Mogab, *J. Amer. Ceram. Soc.*, **52**, 331 (1969).
18. A.H.Heuer, *J. Eur. Ceram. Soc.*, **28**, 1495 (2008).
19. K.P.D.Lagerlof, T.E.Mitchell, A.H.Heuer, *J. Am. Ceram. Soc.*, **72**, 2159 (1989).
20. F.Dwikusuma, T.F.Kuech, *J. Appl. Phys.*, **94**, 5656 (2003).
21. Y.Yan, M.Terauchi, M.Tanaka, *Phil. Mag.*, **A77**, 1027 (1998).
22. A.AlShaikhi, G.P.Srivastava, *J. Appl. Phys.*, **103**, 083554 (2008).
23. M.Akiyama, T.Kamohara, K.Kano et al., *Appl. Phys. Lett.*, **93**, 021903 (2008).
24. G.A.Slack, L.J.Schowalter, D.Morelli, J.A.Freitas, *J. Cryst. Growth*, **246**, 287 (2002).
25. Q.Hu, T.Noda, H.Tanigawa et al., *Nucl. Instr. Meth. Phys. Res.*, **B 191**, 536 (2002).
26. D.Chen, J.Wang, D.Xu, Y.Zhang, *Vacuum*, **83**, 865 (2009).
27. L.Trinkler, L.Botter-Jensen, P.Christensen, B.Berzina, *Radiat. Meas.*, **33**, 731 (2001).

Механізм формування плівок AlN при термохімічній нітридизації сапфиру

Х.Ш.-огли Калтаєв, С.В.Ніжанковський, Н.С.Сідельникова, М.А.Ром, О.Я.Данько, М.В.Добротворська, А.Є.Бєляєв, В.В.Стрельчук, А.Ф.Коломис

Представлені результати досліджень механізму формування плівок AlN на сапфірових підкладинках з орієнтаційними співвідношеннями $(000\bar{1})AlN//(0001)Al_2O_3$, $(0001)AlN//(11\bar{2}0)Al_2O_3$, $(10\bar{1}3)AlN//(1010)Al_2O_3$ і $(11\bar{2}0)AlN//(10\bar{1}2)Al_2O_3$ при термохімічній нітридизації сапфіру у відновних середовищах $N_2 + (CO, H_2)$. Показано, що основні дефекти в отриманих плівках переважно пов'язані з присутністю у них підвищеної концентрації кисню. Обговорюється можливий механізм нітридізації, що включає відновні та дифузійні процеси.